PAPER

UV-VIS spectroscopy for monitoring yogurt stability during storage time

B. Aliakbarian,[a] L. Bagnasco,[b] P. Perego,[a] R. Leardi[b] and M. Casale*[b]

Color, texture and taste are key elements of a consumer's buying decision; thus, monitoring the stability of these features throughout the entire period of yogurt validity is fundamental for dairy product producers. Color, texture and taste deteriorations are due to changes in the physical, chemical and microbiological compositions of yogurt and they can be monitored using lab analyses (especially the microbiological ones) which are expensive and time consuming. In this study, ultraviolet-visible (UV-VIS) spectroscopy was applied as a rapid and alternative technique to traditional analytical methods, to monitor the stability of different commercial yogurt samples up to 49 days of storage at 4 °C. UV-VIS spectroscopy was employed with an integrating sphere for diffuse reflectance measurements and, for each yogurt, color stability during storage time was evaluated in terms of CIEL*a*b* color space values. Moreover, Partial Least Squares regression combined with Genetic Algorithms (GA-PLS) was performed for predicting the age of the yogurt samples from their UV-VIS spectra. In order to evaluate the texture and taste changes, flow curves and pH values of yogurt during storage were monitored once a week for the entire considered storage period. The UV-VIS and rheological datasets were elaborated by means of univariate and multivariate methods. It was interesting to notice that, in both datasets, the time-related information was not visible by simply comparing the profiles of signals, poorly visible in the principal component space, and clearly explained by three-way Principal Component Analysis (3-way PCA).

1. Introduction

Yogurt is a basic dairy product that has been consumed widely as a part of the diet, even when its beneficial effects were neither fully known nor scientifically proven. According to Codex Alimentarius (Codex Stan 243-2003), yogurt is a product obtained by fermentation of milk by means of *Streptococcus thermophilus* and *Lactobacillus delbrueckii* subsp. *bulgaricus*. The function of the starter cultures is to ferment lactose (milk sugar) to produce lactic acid. The increase in lactic acid decreases pH and causes the milk to clot, or form the soft gel that is characteristic of yogurt.[1] The fermentation of lactose also produces the compounds responsible for the typical flavor and acidic conditions restrict the growth of food poisoning pathogens and some spoilage bacteria. Whereas milk has a limited shelf life, yogurt can be kept for up to 20–40 days, under appropriate storage conditions.[2]

Changes in the physical, chemical and microbiological properties of yogurt determine the stability and shelf-life of the product and alterations of these properties cause color, texture and taste deteriorations which are considered important quality

criteria by consumers. As regards the taste, acidity is surely a key parameter to consider.

In the dairy industry, monitoring of products in terms of quality can be performed *via* physicochemical measurements, *i.e.* concentration of target chemicals or biomolecules generally determined by chromatography-mass spectrometry.[3–5] However, these methods are time consuming. The pH and acidity measurements are fast and simple but unfortunately not completely representative of the yogurt modification during storage. The increasing demand for fast, reliable and objective techniques to determine the stability of dairy products during storage encourages scientists to use non-selective analytical techniques, such as spectroscopic methods that are rapid and non-destructive and require a minimal or no sample preparation.

Several researchers have shown the potential of spectroscopic analysis of raw milk in the reflectance, transmittance, or transflectance mode for reliable determination of the fat, protein, and lactose concentration in the laboratory.[6–9] However, since yogurt is a very complex matrix, too dense to allow the measurement of UV-VIS transmittance spectra, reflectance measurements are recommended.

The present study aims at investigating the feasibility of UV-VIS spectroscopy with an integrating sphere for diffuse reflectance measurements as a rapid and alternative technique to traditional analytical methods to monitor the stability of yogurt up to 49 days of storage at 4 °C.

[a] Civil, Chemical and Environmental Engineering Department (DICCA), University of Genoa, Via Opera Pia 15, 16145 Italy

[b] Department of Pharmacy (DIFAR), University of Genoa, Viale Cembrano 4, Genoa, 16148 Italy. E-mail: monica@difar.unige.it; Fax: +39-010-3532684; Tel: +39-010-3532633

In order to reach this goal, Partial Least Squares regression combined with Genetic Algorithms (GA-PLS)[10–12] was performed for predicting the age of the yogurt samples from their UV-VIS spectra and, moreover, color changes during storage were evaluated in terms of CIE$L*a*b*$ color space values (Commission Internationale de l'Eclairage, CIE).[13]

Furthermore, in order to evaluate the texture and taste changes, flow curves and pH values of yogurt during storage were monitored once a week for the entire considered period.

The UV-VIS and rheological datasets were elaborated by means of univariate and multivariate methods in order to extract the useful information.

In this study, the amount of living microorganisms in the product, a key quality parameter regulated by law, was not considered because the main goal was not to investigate the quality of the product. In fact, the quality of the commercial samples that have been chosen is guaranteed by quality controls already carried out by certified laboratories throughout the manufacturing process.

This study represents the first part of a project whose final goal is the addition of natural antioxidants into yogurts. The idea is to follow the behavior of the enriched samples during the storage period using rapid non-destructive analytical tools, in particular the UV-VIS spectroscopy. It was therefore necessary, first, to evaluate the stability of commercial yogurt (*i.e.* without antioxidants) in order to know the behavior of the matrix during storage time and, therefore, to assess the effects that the addition of antioxidants may cause in yogurt.

To the best of our knowledge, this is the first time that reflectance spectroscopy with an integrating sphere was used to monitor the stability of yogurt during storage time.

2. Materials and methods

2.1 Yogurt samples

Eight samples of yogurts produced on the same day (t_0, February 23, 2015) were collected by one of the authors from 4 local dairy farms (indicated as 1, 2, 3 and 4). Five yogurts were full-fat (one was very firm and creamy and one was with blueberries), and three yogurts were fat-free. Each yogurt was split by the producers into eight separate jars, which have been subsequently stored at 4 °C. Every Monday one jar of each yogurt was opened and its content was analysed. This procedure allowed us to monitor the stability of the products during 49 days (t_0, t_1, up to t_7).

Table 1 reports the type, the expiration date (as indicated on the package), and the producer of each yogurt.

Since this was a preliminary feasibility study, the variability between yogurts of the same producer and type was not considered.

2.2 UV-VIS measurements

UV-VIS measurements were performed by placing the yogurt in a 1 cm quartz cuvette in front of the incident light window, and focusing the light reflected from the sample on the detector inside the 60 mm integrating sphere (Agilent, Cary 100, Santa Clara, US). The obtained value is the relative reflectance (with

Table 1 Yogurt samples analysed

Name	Expiration date	Type	Local dairy farm (producer)
HF1	April, 7	White full-fat yogurt	1
HF2	March, 22	White full-fat yogurt	2
HF3	April, 1	White full-fat yogurt	3
HF4	March, 22	White full-fat yogurt very firm and creamy	4
BL1	April, 7	Blueberry full-fat yogurt	1
LF1	April, 2	White fat-free yogurt	1
LF2	March, 22	White fat-free yogurt	2
LF3	April, 1	White fat-free yogurt	3

respect to the reflectance of the reference standard white board, which is taken as 100%). When light is directed at the sample at an angle of 0°, the specular reflected light comes out of the integrating sphere and is not detected; as a result, only diffuse reflected light is measured. Spectra were acquired in the range of 190–900 nm, with spectral bandwidth = 4 nm and average time = 0.1 (a method to improve the signal-to-noise ratio) as suggested by a preliminary 2^2 factorial design (data not shown). The spectral region between 900 and 800 nm was removed because it was not informative; thus, each sample was described by 611 values of reflectance.

The cuvettes were washed with detergent in warm water, accurately rinsed and dried. Three replicates of each sample were recorded and the average signals were taken into account.

2.3 Color analyses in terms of CIE$L*a*b*$ color space values

CIE$L*a*b*$ is the most complete color space specified by the International Commission on Illumination (Commission Internationale de l'Eclairage, CIE). It describes all the colors visible to the human eye and it was created to serve as a device-independent model to be used as a reference.

The three coordinates of CIE$L*a*b*$ represent the lightness of the color ($L* = 0$, no lightness, *i.e.* absolute black, $L* = 100$ diffuse white; specular white may be higher), its position between red/magenta and green ($a*$, negative values corresponding to green and positive values corresponding to magenta) and its position between yellow and blue ($b*$, negative values corresponding to blue and positive values corresponding to yellow).

The difference between two color samples is often expressed as delta E, or ΔE, which describes how far apart visually the two samples are in the color 'sphere'.[14] The ΔE between sample 1 (having L_1^*, a_1^* and b_1^*) and sample 2 (having L_2^*, a_2^* and b_2^*) is:

$$\Delta E = \sqrt{\left(L_2^* - L_1^*\right)^2 + \left(a_2^* - a_1^*\right)^2 + \left(b_2^* - b_1^*\right)^2}$$

Delta E displays the difference as a single value for color and lightness. It is well known that ΔE values less than 3.0 cannot be easily detected by the naked human eye.[15,16] Reflectance spectrophotometers controlled by modern computers such as that used in the present study provide the automatic calculation of the CIE$L*a*b*$ values from the spectral data and the color difference between two spectra.

In this study, in order to evaluate the color stability, for each yogurt, the variations of L^*, a^* and b^* and color difference (ΔE) were calculated matching its spectrum at the initial time (t_0) and its relative spectrum at the expiration date (t_e).

2.4 Flow curves

Rheological properties of different yogurts were measured at 25 °C, once a week, during 49 days of cold storage using a rotational rheometer (RC30, Rheotec Messtechnik GmbH, Berlin, Germany) with a cone-plate geometry (C50-0.4/30). A circulating water bath through the jacket surrounding the plate ensured the temperature control during the analysis. About 2 mL of the sample were used for each measurement.

Shear stress was recorded at increasing shear rates from 0 to 15 s^{-1} at a step of 0.5 s^{-1} (upward flow curve), followed by decreasing shear rates from 15 to 0 s^{-1} at a step of 0.5 s^{-1} (downward flow curve), for a total of 60 points. This limited range of shear rates was chosen in order to support the weak forces present in the inner structure of the yoghurt. The apparent viscosity, calculated as the ratio between the shear stress and shear rate by the Rheo3000 software (Rheotec Messtechnik GmbH, Berlin, Germany), was used for the data elaboration. Since the first and the last points of the shear rate were not taken into account, each sample was described by 58 values of apparent viscosity.

For each sample, three independent subsamples were analysed and their average was taken into account.

2.5 pH measurements

Measurements of pH values of the yogurt samples were performed at 25 °C using a pH-meter model 211 (Hanna Instruments, Woonsocket, USA). For each sample, three independent measurements were performed and data were reported as the mean values of the replicates. pH was measured using an electrode (FC 200 Series, Hanna Instruments, Woonsocket, USA) specific for foods such as milk, yogurt, dairy products, and semi-solid foods.

Before measurements, the pH-meter was calibrated using buffer solutions of HI 7004 (pH 4.01), HI 7007 (pH 7.01) and HI 7010 (pH 10.01).

2.6 Structure of the datasets

Each of the eight samples was analyzed at eight different times, with each analysis producing a data vector. It can therefore be seen how the real structure of the datasets was a parallelepiped whose size was $8 \times J \times 8$, where J was the number of variables: 611 for UV-VIS (reflectance at 611 wavenumbers) and 58 for rheology (apparent viscosity at 29 shear rates for the upward curve and 29 shear rates for the downward curve).

In order to apply standard PCA, these three-way data arrays were matricized to obtain two-way data tables, having 64 rows (8 samples × 8 times) and 611 or 58 columns, respectively.

2.7 Multivariate data analysis

On the previously described datasets, Principal Component Analysis (PCA) and three-way Principal Component Analysis (3-way PCA) were applied as data display methods.

PCA[17] is the most used tool in exploratory data analysis and it uses an orthogonal transformation to convert a set of correlated variables into a set of uncorrelated variables called principal components. Considering the 3-way nature of these matrices, a 3-way PCA was performed by applying the Tucker 3 model.[18] Given an array $\underline{\mathbf{X}}$ of order $I \times J \times K$, Tucker 3 determines component matrices (loadings) for each of the three modes (in our case samples, variables and times, with $I = 8$, $J = 611$ or 58, $K = 8$) and a three-way array $\underline{\mathbf{G}}$ of order $P \times Q \times R$ called the core array, where P is the number of components for the first mode, Q is the number of components for the second mode, and R is the number of components for the third mode. The elements of the core array are the weights for the joint impact of any triplet of components (one from each mode).

The mathematical representation of the Tucker 3 model is:

$$x_{ijk} = \sum_{p=1}^{P} \sum_{q=1}^{Q} \sum_{r=1}^{R} a_{ip} b_{jq} c_{kr} g_{pqr} + e_{ijk}$$

where a_{ip}, b_{jq} and c_{kr} denote elements of the component matrices A, B and C of order $I \times P$, $J \times Q$ and $K \times R$ respectively, g_{pqr} denotes the elements (p, q, r) of the $P \times Q \times R$ core array $\underline{\mathbf{G}}$, and e_{ijk} denotes the error term for element x_{ijk} and is an element of the $I \times J \times K$ array $\underline{\mathbf{E}}$.

The number of factors in each of the three ways is determined by evaluating models with different combinations of components and choosing the solution producing the best compromise between the highest fit and the most parsimonious model. Each of the three sets of loadings can be displayed and interpreted in the same way as a score plot of standard PCA. A joint interpretation of the three sets of loadings can be performed by taking into account the values of the elements of the core matrix.

Data pretreatment is one of the crucial steps in 3-way PCA. To both datasets, a j-scaling[19–21] has been applied. To do that, the three-way array $\underline{\mathbf{X}}$ is matricized to a two-way matrix having $I \times K$ rows and J columns. On it, autoscaling is performed; by doing that, the global variance of each variable is set to one, and the differences among the samples and the times are preserved.

Then, Genetic Algorithms combined with Partial Least Squares regression (GA-PLS) were performed for selecting the UV-VIS bands most informative for predicting the age of the yogurt samples.

Genetic Algorithms (GAs)[10–12] are inspired by Darwin's theory of natural selection. GA-PLS is one of the most commonly used methods for selecting relevant regions in spectroscopic datasets. In our case, since we were interested in detecting the spectral regions related to the evolution in time, the age of the sample was considered as the response to be modeled.

The datasets were analysed with programs developed by the authors in MATLAB (The Mathworks, Natick, MA, USA).

2.8 Statistical analysis

All the experiments were carried out in triplicate ($n = 3$); ANOVA and Tukey's *post-hoc* test ($p < 0.05$) were used ("Statistica 10.0", StatSoft, Tulsa, USA).

3. Results and discussion

3.1 UV-VIS data

3.1.1 Univariate analysis. Fig. 1 shows the UV-VIS spectra relative to one yogurt (sample HF1) for the 8 times (from t_0 to t_7), respectively. It was impossible to depict a spectral region of interest for which a time-dependent trend was apparent since the spectra were completely overlapped.

3.1.2 Principal component analysis. PCA was applied to the auto-scaled UV-VIS spectra as a display method.

The score plot on the plane of the first two components, explaining 96.3% of the total variance (Fig. 2), clearly showed the differences among the three yogurt types, with the blueberry samples (BL1) at highly negative scores on PC1, the full fat samples (HF and BL1) at positive scores of PC2 and the low-fat samples (LF) at negative scores of PC2. As expected, the UV-VIS spectroscopy perfectly distinguished samples with different colors such as the yogurt with blueberries and the white ones.

It was also noted that, for each yogurt, the sample at time t_7 was clearly different from the other times on PC3 (not shown) explaining 3.3% of the total variance. This could indicate that the color of the yogurts (deduced from the spectral features), independent of the period of validity declared by the producer, was approximately constant during the first 5–6 weeks, followed by a sudden modification.

3.1.3 Tucker 3. The optimal number of factors was selected by looking for the best compromise between the highest fit and the most parsimonious model; the model [3 3 2] (3 components for the mode of the samples, 3 components for the mode of variables and 2 components for the mode of the times) explained 99.0% of the total variance of the j-scaled data.

The plot of the loadings of the mode of the samples (first mode, Fig. 3a) was very similar to the PCA score plot (Fig. 2).

The plot of the loadings of the mode of the times (third mode, Fig. 3c) showed a trend on the second factor, with the last time (at which all the eight yogurts were beyond their expiration
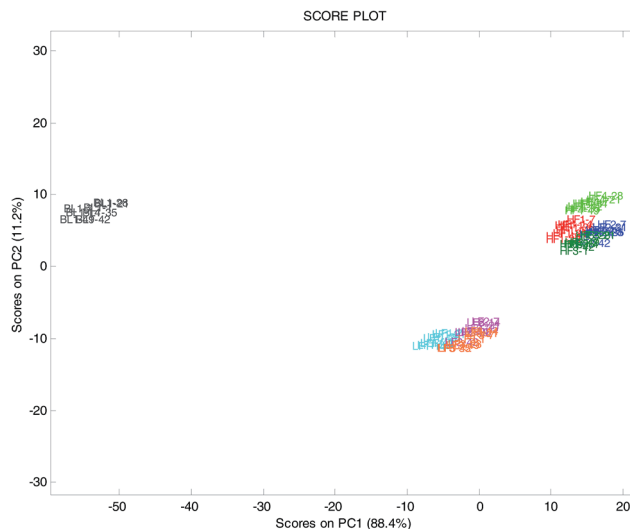

Fig. 1 UV-VIS spectra of yogurt HF1, for the 8 times (t_0–t_7). Reflectance values indicate the relative reflectance with respect to the reflectance of the standard white board (spectralon).

Fig. 2 PCA on the UV-VIS data (64 objects × 611 wavelengths): score plot on the planes PC1–PC2. The samples are coded by the type, the sample number and the storage time (*e.g.*, HF2_14 = high fat yogurt, sample 2, storage time 14 days).

date) very different from the previous ones; this is quite interesting, since it could mean that the UV-VIS data could be used to detect expired products. It has to be noticed that the three-way PCA could detect the time effect much more efficiently than standard PCA.

In order to understand which part of the spectrum is mainly linked to the time effect, the core array (Table 2) must be taken into account. From it one can see that factor 2 of the third mode (times) was mainly related to factor 3 of the second mode (variables), the element [3 3 2] being 33.92. This means that they carried common information and thus can be interpreted jointly.

From the plot of the loadings of the third component of the second mode (Fig. 3b), it can be seen that the region up to 230 nm has high loadings and is therefore related to the time effect.

3.1.4 Prediction of the age of the samples. PLS was performed in order to check if it was possible to predict the age of the sample from its spectrum. The elaboration was performed both on the whole spectra and on subsets of variables chosen by the Genetic Algorithm (GA) as the bands most informative in defining the time effect.

3.1.4.1 Whole spectra. PLS was performed on the whole spectra; the optimal complexity of the PLS models, *i.e.* the number of latent variables (LV), was chosen on the basis of the explained variance in cross-validation (Venetian blinds, 5 deletion groups); the models were calculated at the optimal LV number and the standard error in prediction (SEP) was finally obtained, using an independent external test set with 16 spectra (2 for each time) randomly selected.

Fig. 4 shows the experimental *versus* the predicted response (days of storage, from 0 to 49) for the external test set; the performances of this model were quite satisfactory with a SEP of 3.3 days and a bias of −0.1 days.

3.1.4.2 Variables selected by GA. The application of GA allowed the detection of three spectral regions related to the time effect: 210–230 nm, 300–350 nm and 480–570 nm.
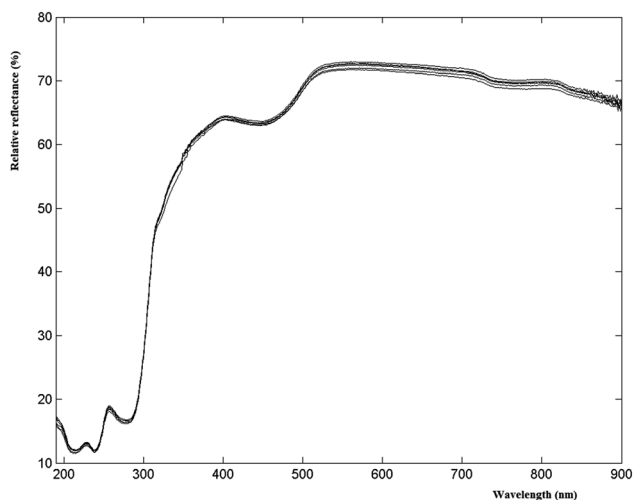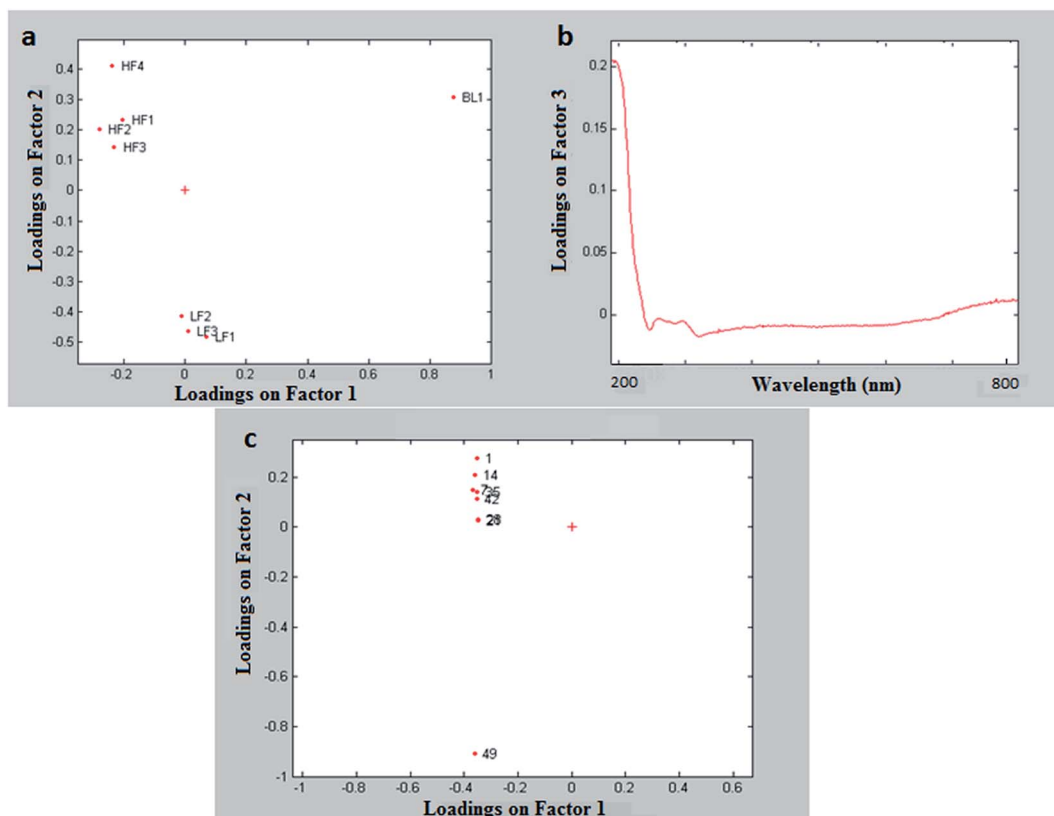
Fig. 3 UV-VIS data: Tucker 3 model; (a) first mode (yogurts) and loadings on the plane factor 1 *vs.* factor 2, (b) second mode (variables) and loadings on factor 3; (c) third mode (times), and loadings on the plane factor 1 *vs.* factor 2.

Table 2 Core array of the Tucker 3 model [3 3 2] on the UV-VIS data

$g(:,:,1)$		
−180.37	0.15	−0.67
0.05	65.57	3.59
0.15	−1.79	−0.48

$g(:,:,2)$		
−0.14	0.69	−0.66
1.12	−0.26	−3.46
3.45	6.98	−33.92

Many compounds can produce these absorptions but the ones responsible for the modifications of yogurt during storage time are especially due to protein structural changes, whose absorptions interest these regions.[22]

The performances of the PLS model built on the selected variables were slightly better than the ones of the model obtained using the whole spectra (SEP: 3.0 days; bias: −0.1 days).

It was also interesting to notice that the selection of the first region (210–230 nm) was in full agreement with the results obtained with the Tucker 3 model.

3.2 Rheological data

3.2.1 Univariate analysis. Fig. 5 shows the flow curves relative to one yogurt (sample HF1) for the 8 times, respectively.
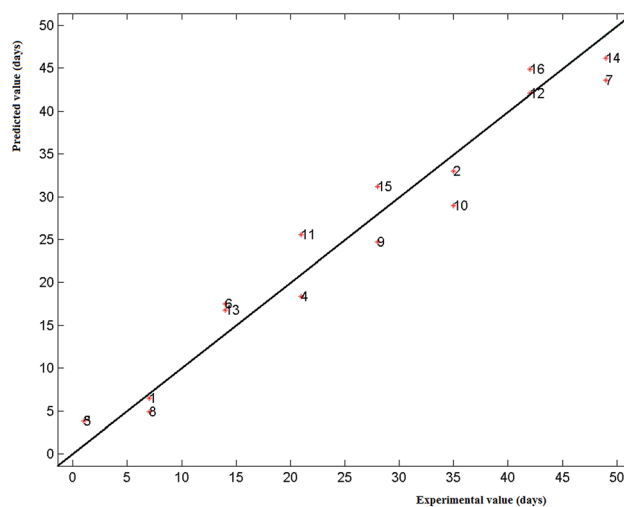

Fig. 4 UV-VIS data: PLS model on the whole spectra; experimental *vs.* predicted values (days of storage) for the external test set samples (16 samples randomly selected).

In the first phase of the upward curve, up to 50–80 Pa (depending on the storage time), yogurt behaved as an elastic solid; at higher shear rates at first it underwent some distortion and it was broken into small pieces showing a viscoelastic behavior. This was in accordance with the
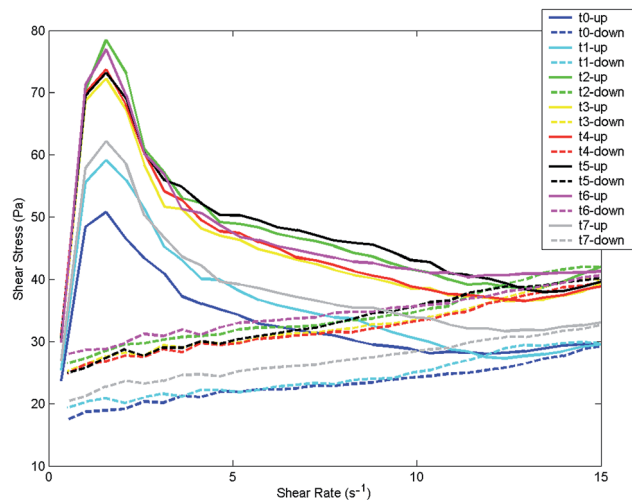
Fig. 5 Rheological data: flow curves (upward and downward) of yogurt HF1, for the 8 storage times (t_0-t_7).

observation reported by Tulay Ozcan[23] who affirmed that yogurt's rheological properties can be characterized using both the viscous and elastic components. Viscoelasticity indicates that the material has some of the elastic properties of an ideal solid and some of the flow properties of an ideal (viscous) liquid.[24]

It has to be noticed that the visual analysis of the flow curves recorded at different storage times does not allow the detection of a time related effect.

Table 3 shows the apparent viscosity of samples at a shear rate of 1 s^{-1} during the storage period.

Apparent viscosity resulted in the increase in almost all samples (except for HF2) with significant statistical differences ($p < 0.05$). This increase was more evident (174%) in the case of LF3, in which apparent viscosity was the lowest when compared to that of all other samples (from 3.10 Pa s to 8.49 Pa s after 49 days of cold storage). The increase in the apparent viscosity during storage can be attributed to the syneresis, protein hydration and exopolysaccharide production. The same

influence of storage time on the viscosity of yogurt stored at 4 °C for 14 days was noticed by Afonso and Maia[25] when they used cooled stirred samples. In another study, Abu-Jdayil and Mohameed[26] noticed an increase of apparent viscosity of labneh (concentrated yogurt) during storage time. Their explanation was attributed to the protein rearrangement and gel development during the storage period.

3.2.2 Principal component analysis. PCA was performed on the autoscaled data. The first principal component explained almost the total variance of the dataset (99.8%), and, as expected, mainly showed the difference between the very firm full-fat yogurt and the other samples.

Also looking at the lower components, or removing the very different sample, it was not possible to detect any time effect (data not shown).

3.2.3 Tucker 3. For rheological data, the model [2 1 2] explained 98.81% of the total variance of the j-scaled data.

As expected, the very firm and creamy yogurt (sample HF4) was very different from the other ones on the first factor of the first mode (Fig. 6a). It was also interesting to see that samples from the same producer (i.e.: HF1, LF1 and BL1) had similar loadings on the first factor this meaning that it is related to the effect of the producer. The second factor showed instead the difference between low-fat and high-fat samples. In spite of the fact that the two types of yogurt were not clearly separated along this factor, it could anyway be seen that for every producer the loading of the low-fat sample was more negative than the loading of the corresponding high-fat sample.

The time effect was shown clearly on the second factor of the third mode (Fig. 6b). This effect was not visible in the PCA because its magnitude was much smaller than the magnitude of the effect of the samples. Instead, the Tucker 3 model was capable of extracting it independently from the other sources of variation. It was interesting to notice that the "structure" of the yogurt changed regularly with time, with the greatest variation occurring in the first week after its production. This information is complementary to what has been found with the UV-VIS data, which highlighted variations occurring after the expiration date.

Table 3 Apparent viscosity (Pa s) of different yogurt samples at a shear rate of 1 s^{-1} during the storage at 4 °C^a

	Storage time (weeks)							
Sample	t_0	t_1	t_2	t_3	t_4	t_5	t_6	t_7
HF1	11.25 ± 1.04[c]	17.08 ± 1.12[ab]	16.61 ± 0.50[ab]	14.42 ± 0.56[b]	18.52 ± 0.41[a]	17.36 ± 0.51[a]	18.32 ± 0.96[a]	16.76 ± 1.82[ab]
HF2	9.72 ± 1.56[ab]	8.35 ± 0.47[a]	8.96 ± 0.51[ab]	8.96 ± 1.39[ab]	10.64 ± 0.54[ab]	10.26 ± 0.32[ab]	10.77 ± 0.21[b]	8.34 ± 0.21[a]
HF3	9.10 ± 1.35[a]	10.58 ± 1.20[ab]	9.46 ± 0.41[a]	10.40 ± 0.61[ab]	12.94 ± 1.13[bc]	13.92 ± 0.84[c]	13.24 ± 1.37[bc]	11.02 ± 1.11[abc]
HF4	44.95 ± 3.77[c]	61.63 ± 6.80[b]	75.95 ± 2.29[a]	69.05 ± 2.26[ab]	75.64 ± 5.92[a]	72.57 ± 3.83[ab]	77.19 ± 2.60[a]	61.41 ± 2.54[b]
BL1	9.89 ± 1.68[c]	11.59 ± 0.24[ac]	12.01 ± 0.40[ac]	13.68 ± 1.10[ab]	17.06 ± 1.57[b]	16.22 ± 2.12[b]	13.58 ± 1.62[abc]	13.96 ± 0.28[ab]
LF1	9.27 ± 0.79[b]	13.38 ± 1.94[ab]	14.19 ± 0.25[a]	12.89 ± 1.15[ab]	15.09 ± 3.88[a]	15.13 ± 0.30[a]	14.67 ± 1.03[a]	12.90 ± 0.44[ab]
LF2	9.15 ± 3.70[b]	11.84 ± 1.10[ab]	13.13 ± 3.16[ab]	13.79 ± 1.94[ab]	13.53 ± 1.19[ab]	17.13 ± 0.98[b]	17.6 ± 6 0.72[b]	12.1 ± 2.33[ab]
LF3	3.10 ± 1.31[d]	6.87 ± 0.36[ab]	6.32 ± 0.85[ab]	7.19 ± 0.56[abc]	5.82 ± 1.33[b]	8.50 ± 0.67[ac]	9.46 ± 1.08[c]	8.49 ± 0.13[ac]

^{a} ± indicates standard deviations with respect to the mean values of triplicate measurements. Different letters within the rows indicate significant statistical differences between data during storage at $p < 0.05$.
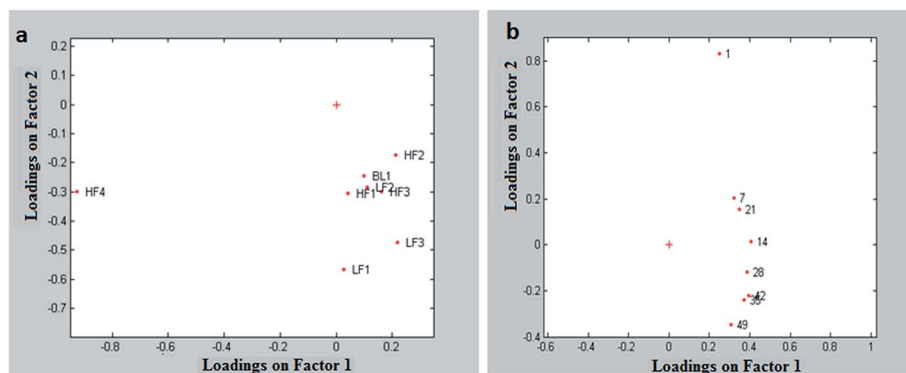
Fig. 6 Rheological data: Tucker 3 model; (a) first mode (yogurts) and loadings on the plane factor 1 *vs.* factor 2; (b) third mode (times) and loadings on the plane factor 1 *vs.* factor 2.

3.3 Color and pH analyses

Table 4 lists, for each yogurt, the variations of the color coordinates L^*, a^* and b^* and ΔE between the initial time (t_0) and the expiration date (t_e).

The variations of L^*, a^* and b^*, except for the blueberry yogurt, were minimal, in general lower than 1. It was interesting to notice that full-fat and fat-free yogurts showed a different trend: full-fat samples had L^* values slightly higher and during storage they became redder/bluer. In contrast, the fat-free samples tended to become greener/yellower.

Table 4 Variations of L^*, a^* and b^* and color difference (ΔE) of each yogurt between the initial time (t_0) and the expiration date (t_e)

Sample	$L^*(t_0)$	$L^*(t_e)$	$a^*(t_0)$	$a^*(t_e)$	$b^*(t_0)$	$b^*(t_e)$	$\Delta E(t_0 - t_e)$
HF1	65.65	64.66	−9.42	−9.34	29.19	28.78	1.07
HF2	66.08	64.79	−9.11	−8.87	22.81	22.53	1.34
HF3	65.74	65.36	−8.89	−8.76	23.20	22.88	0.95
HF4	65.86	67.14	−8.95	−9.03	29.05	29.56	1.38
BL1	49.01	53.47	67.88	60.69	−7.61	−2.37	9.95
LF1	63.43	63.39	−14.06	−14.61	30.63	30.67	0.55
LF2	63.65	64.68	−10.66	−11.05	18.51	19.47	1.46
LF3	63.62	63.26	−9.74	−10.32	16.75	17.38	0.93

All the white yogurts showed ΔE values lower than 3, not appreciated at first glance by the human eye; in contrast, blueberry yogurt showed a higher ΔE value (9.95), indicating that the change of color was visible to an untrained person. It is also interesting to notice that for all the yogurts the ΔE values calculated matching the spectrum at the expiration date (t_e) and the spectrum of the same yogurt at the final time (t_7) were higher than 3 (not reported).

This was in total agreement with the results of the PCA on the UV-VIS data, meaning that the product was quite stable throughout the whole validity period, and then it underwent a quite fast degradation.

Table 5 shows the pH changes of each yogurt during the storage period, where each value is the average of 3 measurements. The highest decrease in pH (from 4.33 ± 0.02 to 4.18 ± 0.02) was noticed for sample HF4 (the sample with the highest initial pH) with statistical differences ($p < 0.05$) passing from t_0 to t_7. Blueberry yogurt (sample BL1) was characterized by higher acidity due to the addition of the fruit preparation. Changes in pH were more evident ($p < 0.05$) during the first week of storage. This agrees with the results obtained on the rheological data and similar findings were also reported by Salji and Ismail[27] for plain yogurt stored at 4 °C for three weeks.

Table 5 Changes in pH values of different yogurt samples during storage at 4 °C[a]

Sample	Storage time (weeks)							
	t_0	t_1	t_2	t_3	t_4	t_5	t_6	t_7
HF1	4.11 ± 0.02^a	3.99 ± 0.01^{bc}	4.12 ± 0.01^a	4.07 ± 0.02^a	3.97 ± 0.03^c	3.99 ± 0.04^{bc}	4.05 ± 0.03^{ab}	4.06 ± 0.02^{ab}
HF2	4.08 ± 0.02^b	3.99 ± 0.02^a	4.07 ± 0.02^b	3.79 ± 0.05^c	4.04 ± 0.02^{ab}	4.01 ± 0.01^a	4.05 ± 0.02^{ab}	4.04 ± 0.02^{ab}
HF3	3.95 ± 0.01^{bc}	3.94 ± 0.01^{ab}	4.05 ± 0.03^d	3.97 ± 0.01^c	3.93 ± 0.01^{ab}	3.90 ± 0.02^a	4.06 ± 0.01^d	3.94 ± 0.02^{ab}
HF4	4.33 ± 0.02^d	4.22 ± 0.01^{abc}	4.25 ± 0.03^c	4.17 ± 0.10^b	4.24 ± 0.01^{ac}	4.19 ± 0.01^{ac}	4.18 ± 0.03^{ab}	4.18 ± 0.02^{ab}
BL1	3.68 ± 0.02^d	3.60 ± 0.01^{abc}	3.65 ± 0.01^{bcd}	3.65 ± 0.03^{cd}	3.62 ± 0.01^{abcd}	3.57 ± 0.03^a	3.57 ± 0.04^{ab}	3.64 ± 0.04^{abcd}
LF1	3.97 ± 0.02^e	3.85 ± 0.01^{ab}	3.91 ± 0.01^{cd}	3.84 ± 0.01^{ab}	3.93 ± 0.02^c	3.83 ± 0.02^a	3.87 ± 0.02^{bd}	3.92 ± 0.01^c
LF2	4.12 ± 0.02^{ab}	4.08 ± 0.02^a	4.12 ± 0.01^{ab}	4.09 ± 0.01^{ab}	4.12 ± 0.01^{ab}	4.08 ± 0.03^a	4.07 ± 0.03^a	4.15 ± 0.02^b
LF3	4.02 ± 0.01^d	3.93 ± 0.01^a	3.99 ± 0.02^{bc}	4.02 ± 0.20^{cd}	3.98 ± 0.02^b	3.92 ± 0.02^a	4.01 ± 0.02^{bcd}	3.94 ± 0.01^a

[a] $\pm$ indicates standard deviations with respect to the mean values of triplicate measurements. Different letters within the rows indicate significant statistical differences between data during storage at $p < 0.05$.

4. Conclusions

Color, texture and taste are key elements of a consumer's acceptance; thus, monitoring the stability of these features throughout the entire period of yogurt validity is fundamental for dairy product producers.

The UV-VIS spectrum contains chemical information and can also be used for color stability evaluation. Therefore, in this study, diffuse reflectance UV-VIS spectroscopy was applied as a rapid and alternative technique to traditional analytical methods to evaluate the changes of different commercial yogurts up to 49 days of storage at 4 °C. Flow curves and pH values of yogurt during storage were also monitored once a week for the entire considered period, in order to evaluate the texture and taste stability, respectively.

As far as the UV-VIS spectra are concerned, by using Tucker 3, it was possible to distinguish among white full-fat, white fat-free yogurts and, as expected, the blueberry full-fat yogurt (first mode), to identify the UV-VIS regions related to the time effect (second mode) and to detect the time effect (third mode).

Moreover, the ΔE values calculated matching the spectrum of each white yogurt at the initial time (t_0) and its spectrum at the expiration date (t_e) were lower than 3, indicating color variations not appreciated by the human eye; after the expiration date in contrast, the ΔE values were always higher indicating variations in color visible also for untrained personnel. This was in agreement with the loadings of the third mode of the Tucker 3 model for the UV-VIS spectra, showing that the last time was very different from the other ones. By applying a multivariate calibration, it was also possible to predict acceptably well the age of the yogurt samples from the UV-VIS spectra.

As far as the rheological data are concerned, the loadings of the third mode of the Tucker 3 model showed a trend over time. It was interesting to notice that the information contained in the rheological data was not visible comparing the profiles of signals during time, poorly visible in the principal component space, and well explained by the 3-way model.

Finally, it has to be noticed that the different analytical methods provided complementary information.

The results of this study are fundamental for the second part of a project whose final scope is the addition of natural antioxidants into yogurts. In order to monitor the antioxidant-rich samples during the storage period using UV-VIS spectroscopy, it was necessary to perform a previous evaluation of the stability of commercial yogurt (*i.e.* without antioxidants); in this way it will be possible to assess the effects that the addition of antioxidants may cause in yogurt.

Acknowledgements

References

1 W. Routray and H. N. Mishra, *Compr. Rev. Food Sci. Food Saf.*, 2011, **10**, 208–220.
2 A. Sofu and F. Y. Ekinci, *J. Dairy Sci.*, 2007, **90**, 3118–3125.
3 A. M. Mortazavian, K. Rezaei and S. Sohrabvandi, *Crit. Rev. Food Sci. Nutr.*, 2009, **49**, 153–163.
4 K. Gaus, P. Rösch, R. Petry, K.-D. Peschke, O. Ronneberger, H. Burkhardt, K. Baumann and J. Popp, *Biopolymers*, 2006, **82**, 286–290.
5 C. Carrillo-Carrión, S. Cárdenas and M. Valcárcel, *J. Chromatogr. A*, 2007, **1141**, 98–105.
6 M. F. Laporte and P. Paquin, *J. Agric. Food Chem.*, 1999, **47**, 2600–2605.
7 R. Tsenkova, S. Atanassova, S. Kawano and K. Toyoda, *J. Anim. Sci.*, 2001, **79**, 2550–2557.
8 R. S. Jankovska, *Czech J. Food Sci.*, 2003, **21**, 123–128.
9 B. Aernouts, E. Polshin, J. Lammertyn and W. Saeys, *J. Dairy Sci.*, 2011, **94**, 5315–5329.
10 R. Leardi and A. Lupiáñez González, *Chemom. Intell. Lab. Syst.*, 1998, **41**, 195–207.
11 Z. Xiaobo, Z. Jiewen, M. J. W. Povey, M. Holmes and M. Hanpin, *Anal. Chim. Acta*, 2010, **667**, 14–32.
12 R. Leardi, *J. Chemom.*, 2000, **14**, 643–655.
13 A. D. Broadbent, *Color Res. Appl.*, 2004, **29**, 267–272.
14 N. Guven and P. Camurlu, *Polymer*, 2015, **73**, 122–130.
15 S. I. Hong, J. H. Han and J. M. Krochta, *J. Appl. Polym. Sci.*, 2004, **92**, 335–343.
16 P. Cerezal Mezquita, B. E. Barragán Huerta, J. C. Palma Ramírez and C. P. Ortíz Hinojosa, *J. Food Sci. Technol.*, 2015, **52**, 1634–1641.
17 D. L. Massart, B. G. M. Vandeginste, L. M. C. Buydens, S. De Jong, P. L. Lewi and J. Smeyers-Verbeke, in *Handbook of Chemometrics and Qaulimetrics: Part B*, ed. B. G. M. Vandeginste and S. C. Rutan, Elsevier, 1998, pp. 88–103.
18 L. R. Tucker, *Psychometrika*, 1966, **31**, 279–311.
19 R. Henrion, *Chemom. Intell. Lab. Syst.*, 1994, **25**, 1–23.
20 P. J. Gemperline, K. H. Miller, T. L. West, J. E. Weinstein, J. C. Hamilton and J. T. Bray, *Anal. Chem.*, 1992, **64**, 523A–532A.
21 R. Henrion and C. A. Andersson, *Chemom. Intell. Lab. Syst.*, 1999, **47**, 189–204.
22 S. M. Loveday, J. P. Hindmarsh, L. K. Creamer and H. Singh, *Food Res. Int.*, 2009, **42**, 798–806.
23 T. Ozcan, *2nd International Conference on Nutrition and Food Sciences, IPCBEE*, IACSIT Press, 2013, vol. 53.
24 J. F. Steffe, *Rheological methods in food process engineering*, Freeman Press, 1996.
25 I. M. Afonso and J. M. Maia, *J. Food Eng.*, 1999, **42**, 183–190.
26 B. Abu-Jdayil and H. Mohameed, *J. Food Eng.*, 2002, **52**, 359–365.
27 J. P. Salji and A. A. Ismail, *J. Food Sci.*, 1983, **48**, 258–259.